




## RESEARCH ARTICLE

# The appendicularian *Oikopleura dioica* can enhance carbon export in a high CO<sub>2</sub> ocean

Jan Taucher<sup>1</sup>  | Anna Katharina Lechtenbörger<sup>1</sup> | Jean-Marie Bouquet<sup>2,3</sup> | Carsten Spisla<sup>1</sup> | Tim Boxhammer<sup>1</sup> | Fabrizio Minutolo<sup>1,4</sup> | Lennart Thomas Bach<sup>5</sup>  | Kai T. Lohbeck<sup>6</sup> | Michael Sswat<sup>1</sup>  | Isabel Dörner<sup>1</sup> | Stefanie M. H. Ismar-Rebitz<sup>1</sup> | Eric M. Thompson<sup>2,3</sup> | Ulf Riebesell<sup>1</sup>

<sup>1</sup>GEOMAR Helmholtz Centre for Ocean Research Kiel, Kiel, Germany

<sup>2</sup>Department of Biological Sciences, University of Bergen, Bergen, Norway

<sup>3</sup>Michael Sars Centre for Marine Molecular Biology, University of Bergen, Bergen, Norway

<sup>4</sup>Institute of Carbon Cycles, Helmholtz-Centre Hereon, Geesthacht, Germany

<sup>5</sup>Institute for Marine and Antarctic Studies, University of Tasmania, Hobart, Tasmania, Australia

<sup>6</sup>Limnological Institute, University of Konstanz, Konstanz, Germany

## Correspondence

Jan Taucher, GEOMAR Helmholtz Centre for Ocean Research Kiel, Kiel, Germany. Email: [jtaucher@geomar.de](mailto:jtaucher@geomar.de)

## Funding information

Deutsche Forschungsgemeinschaft; Norges Forskningsråd, Grant/Award Number: NFR-HK 204040

## Abstract

Gelatinous zooplankton are increasingly recognized to play a key role in the ocean's biological carbon pump. Appendicularians, a class of pelagic tunicates, are among the most abundant gelatinous plankton in the ocean, but it is an open question how their contribution to carbon export might change in the future. Here, we conducted an experiment with large volume in situ mesocosms (~55–60 m<sup>3</sup> and 21 m depth) to investigate how ocean acidification (OA) extreme events affect food web structure and carbon export in a natural plankton community, particularly focusing on the keystone species *Oikopleura dioica*, a globally abundant appendicularian. We found a profound influence of *O. dioica* on vertical carbon fluxes, particularly during a short but intense bloom period in the high CO<sub>2</sub> treatment, during which carbon export was 42%–64% higher than under ambient conditions. This elevated flux was mostly driven by an almost twofold increase in *O. dioica* biomass under high CO<sub>2</sub>. This rapid population increase was linked to enhanced fecundity (+20%) that likely resulted from physiological benefits of low pH conditions. The resulting competitive advantage of *O. dioica* resulted in enhanced grazing on phytoplankton and transfer of this consumed biomass into sinking particles. Using a simple carbon flux model for *O. dioica*, we estimate that high CO<sub>2</sub> doubled the carbon flux of discarded mucous houses and fecal pellets, accounting for up to 39% of total carbon export from the ecosystem during the bloom. Considering the wide geographic distribution of *O. dioica*, our findings suggest that appendicularians may become an increasingly important vector of carbon export with ongoing OA.

## KEYWORDS

biological carbon pump, carbon fluxes, gelatinous zooplankton, global change, larvaceans, mesocosm experiments, ocean acidification

This is an open access article under the terms of the [Creative Commons Attribution-NonCommercial-NoDerivs](https://creativecommons.org/licenses/by-nc-nd/4.0/) License, which permits use and distribution in any medium, provided the original work is properly cited, the use is non-commercial and no modifications or adaptations are made.

© 2023 The Authors. *Global Change Biology* published by John Wiley & Sons Ltd.

## 1 | INTRODUCTION

### 1.1 | The role of appendicularians in the biological pump

The flux of sinking organic matter from the surface to the deep ocean is a key mechanism in the oceanic carbon cycle. This “biological pump” is essential in supplying food to deep-sea biota, as well as in transferring carbon to the ocean interior and thereby regulating atmospheric CO<sub>2</sub> (Boyd et al., 2019; Volk & Hoffert, 1985). Large uncertainties still remain about the mechanisms driving the biological pump, particularly regarding the role of food web structure and different zooplankton taxa in regulating carbon export (Boyd et al., 2019; Burd et al., 2016). One crucial knowledge gap is the role of gelatinous zooplankton, a diverse taxonomic group (comprising cnidarians, ctenophores, and pelagic tunicates) that has recently experienced a growing recognition as a potentially important component of the biological pump (Jaspers et al., 2023; Luo et al., 2020; Steinberg et al., 2023).

Appendicularians are pelagic tunicates that are often considered to be the second-most abundant mesozooplankton group in the ocean, after copepods (Gorsky & Fenaux, 1998; Hopcroft & Roff, 1998; Jaspers et al., 2023) (and during blooms even exceeding copepod abundances; Questel et al., 2013). Appendicularians feed efficiently and at high rates, mostly on small particles in the pico- and nanoplankton size range (Flood, 1978; Lombard et al., 2011). Their population dynamics display typical boom-and-bust characteristics, that is, high grazing rates in combination with a short generation time and life cycle, allowing them to develop intense blooms (Hopcroft & Roff, 1995; Nakamura et al., 1997; Sato et al., 2008). The most prominent feature of appendicularians is their mucous feeding structure (“house”), which is produced and discarded several times per day, usually still including a large portion of filtered but non-ingested particles, as well as fecal pellets (Lombard, Sciandra, et al., 2009; Sato et al., 2001). Sinking velocities of discarded houses are comparatively high (up to several hundred meters per day, also depending on ballast; Lombard et al., 2013) and often collect additional particles while sinking to depth due to their stickiness (Alldredge, 2005; Hansen et al., 1996; Lombard et al., 2013).

Due to these peculiar characteristics, appendicularians are thought to play an important role in carbon export and the biological pump (Jaspers et al., 2023). However, quantifying this role has remained difficult, let alone achieving a mechanistic understanding of how appendicularian blooms influence pelagic food web structure and carbon export. A major reason is that appendicularians (as all gelatinous taxa) are fragile and often destroyed during conventional net sampling, resulting in systematic biases and underestimation of their biomass (of up to 10-fold) (Luo et al., 2014; Remsen et al., 2004). Another challenge is the fact that blooms of appendicularians (and tunicates in general) are usually patchy and short-lived, with associated carbon export occurring in short pulses (Alldredge, 2005; Stone & Steinberg, 2016; Vargas et al., 2002). Capturing this substantial spatial and temporal variability with ship-based observations is very challenging, as such surveys are

usually conducted along transects but do not track water masses in a Lagrangian manner. Instead, most existing observations of appendicularian blooms (and those of other pelagic tunicates) and associated export events during ship cruises were collected rather coincidentally and did not allow examining temporal dynamics and the contribution of appendicularian blooms to food web structure and carbon export in detail. Despite these limitations, previous studies suggest that the contribution of appendicularians to total carbon export can be substantial (mainly via discarded houses), but also display a high degree of variability and uncertainty, with observation-based estimates reaching from around 10% to more than 80% of total particulate carbon export across several oceanic and coastal regions (Alldredge, 2005; Berline et al., 2010; Vargas et al., 2002; Wilson et al., 2013).

### 1.2 | The influence of ocean acidification on *O. dioica*

An improved understanding of the role of appendicularians (and gelatinous zooplankton in general) in pelagic food webs and biogeochemical cycling requires robust empirical data on population dynamics and carbon fluxes, particularly considering changing environmental conditions in the future ocean.

One of the major knowledge gaps is how ocean acidification (OA) may alter the role of appendicularians in driving carbon export, particularly during extreme acidity events, that is, periods of very low pH that are expected to increase in frequency, duration, and amplitude in the future ocean (Burger et al., 2020; Gruber et al., 2021; Kwiatkowski & Orr, 2018). Physiological experiments with the cosmopolitan appendicularian species *Oikopleura dioica* demonstrated enhanced fecundity under OA (i.e., higher egg production), which could be a potential competitive advantage over other zooplankton species (Bouquet et al., 2018; Troedsson et al., 2013; Winder et al., 2017). However, experiments with natural communities have demonstrated that community-level impacts of OA are usually far more complex and variable than expected from single-species responses observed in controlled laboratory experiments, for example, due to the combination of direct physiological effects and indirect effects mediated through the food web (Goldenberg et al., 2018; Sswat et al., 2018; Taucher et al., 2020).

In this study, we assessed whether high CO<sub>2</sub> conditions as expected for future OA extreme events could benefit *O. dioica* in a natural plankton community and how that would affect carbon export.

## 2 | METHODS

### 2.1 | In situ mesocosm experiment

We conducted an experiment with eight pelagic in situ mesocosms (~60 m<sup>3</sup>) in a temperate ocean region (Raunefjord, Norway) over a period of 8 weeks from May to June 2015. For a comprehensive description of experimental design and technical details, please refer to Spisla et al. (2021). Briefly, the setup consisted of eight pelagic

mesocosms (M1–M8), each extending to a depth of 21 m (19 m cylindrical bag and 2 m full size/diameter conical sediment trap attached to the bottom of the bag) and enclosing about 60 m<sup>3</sup> of the natural water column. Four mesocosms were maintained at ambient conditions, while carbonate chemistry was manipulated in the other four mesocosms (high CO<sub>2</sub> treatment).

Average  $p\text{CO}_2$  during the experiment ranged between ~320 ("ambient") and 1700  $\mu\text{atm}$  ("high CO<sub>2</sub>," corresponding to a drop in pH by 0.57 units compared to ambient conditions). We chose such a high magnitude of carbonate chemistry perturbation to simulate a future OA extreme event, that is, episodic extremes of carbonate chemistry (on weekly to monthly timescales) that are superimposed onto the long-term decadal- to centennial-scale progression of OA. Such periods of very low pH already occur under present-day conditions in some ocean regions, reaching drops in pH by 0.2–0.5 units and corresponding changes in carbonate chemistry (Desmet et al., 2022; Hauri et al., 2013). Recent work has shown that such extreme acidity events will markedly increase in amplitude and duration in the future ocean (Burger et al., 2020; Gruber et al., 2021; Kwiatkowski & Orr, 2018). Furthermore, carbonate chemistry conditions that would be considered as extreme events in the near future could be reached on a global average near the end of the 22nd century under high-emission scenarios (RCP8.5) (Meinshausen et al., 2011).

In our experiment, the OA treatment was established by injecting CO<sub>2</sub>-enriched seawater into four of the eight mesocosm enclosures following the method described in Riebesell et al. (2013). Natural seawater was enriched with pure CO<sub>2</sub> gas in a large mixing tank, filled into 20 L bottles, and added to the mesocosms with a special distribution device to ensure homogenous CO<sub>2</sub> enrichment throughout the entire water column. CO<sub>2</sub> enrichment was carried out in the initial phase (gradual  $p\text{CO}_2$  increase between days 1 and 6), plus five times throughout the experiment (days 14, 22, 28, 40, and 46) to maintain carbonate chemistry within target levels. Average  $p\text{CO}_2$  during the experiment ranged between ~320 and 1700  $\mu\text{atm}$  in the ambient and "high CO<sub>2</sub>" mesocosms, respectively.

Throughout the study period of 55 days, the enclosed water column was sampled regularly for a comprehensive set of physical, chemical, and biological parameters. A conical sediment trap attached to the bottom of the mesocosms collected the particulate material sinking out of the water column.

## 2.2 | Abundance, biomass, and fecundity (egg production) of *O. dioica*

Net hauls specifically targeting appendicularians were conducted with a special approach, as these organisms (as many other gelatinous zooplankton taxa) are very fragile and therefore require special caution to avoid damage by net sampling (Luo et al., 2022; Remsen et al., 2004). Therefore, a custom-built net (50  $\mu\text{m}$  mesh size; 20 cm in diameter) with a modified, non-filtering cod end (3.8 L clear polycarbonate beaker) and reduced towing speeds (0.15 m s<sup>-1</sup>) was applied in order to collect alive and undamaged *O. dioica* specimen.

Furthermore, a high temporal sampling frequency of 4 days was chosen for these appendicularian net hauls, taking into consideration that *O. dioica* is a semelparous organism with a short life cycle of about 10–12 days at the in situ temperatures in this study (Bouquet, 2017; Lombard, Sciadra, et al., 2009). A subsample of 500–1000 mL was filtered through a 70- $\mu\text{m}$  mesh and transferred to a glass dish, where organisms were microscopically identified and counted, using a microscope (Olympus SZX2-ZB16) equipped with a Nikon camera (DS-5M) connected to a Nikon system (DS-L1) and Image Pro Plus (Version 4.5.0.29). Furthermore, individuals of *O. dioica* (without their houses) were photographed for measurements of trunk length (excluding gonads;  $n=8283$  for the entire study period). Carbon biomass of *O. dioica* was calculated using the relationship between trunk length and body mass from Lombard, Renaud, et al. (2009).

Subsamples were used for culture experiments to examine fecundity of *O. dioica* under ambient and OA conditions. Therefore, female *O. dioica* were cultured in mesocosm water (pre-filtered through a 50- $\mu\text{m}$  mesh) of the respective CO<sub>2</sub> conditions until they achieved maturity and produced eggs. Incubations were conducted in special beakers (8-L clear polycarbonate), kept at temperature and pH levels corresponding to those in the mesocosms, and were maintained for 2–4 days after sampling. Each beaker was equipped with a continuous rotating "paddle" to ensure gentle and sufficient mixing of the water without damaging the delicate body structures of *O. dioica* (Bouquet et al., 2009). The culture beakers were checked several times a day for females close to spawning. All mature females close to spawning were then separated into a glass petri dish and the eggs were photographed immediately after spawning with a camera connected to a microscope (Olympus SZX2-ZB16) for subsequent counting. Fecundity data were analyzed by computing probability densities based on kernel density estimation, as this method better accounts for data with skewed or multimodal distributions compared to classical pairwise tests (Schartau et al., 2010). Confidence intervals of the density estimates were calculated with a bootstrapping approach using data resampling (1000 permutations) (Schartau et al., 2010). The resulting probability density plots can be interpreted analogously to histograms. Differences among ambient and high CO<sub>2</sub> conditions are considered statistically significant when confidence intervals of the probability density distributions do not overlap.

## 2.3 | Abundance and biomass of other mesozooplankton

Mesozooplankton samples were collected every 8 days using an Apstein net with 55  $\mu\text{m}$  mesh size and a 17 cm diameter cone-shaped opening. Net catches were collected by vertical tows (~0.5 m s<sup>-1</sup>) from 19 m depth up to the surface, corresponding to a sampling volume of 431 L per net haul. Samples were preserved in 70% EtOH. Prior to counting, the samples were split with a Folsom plankton splitter to one-eighth of the original sample. Starting with the first aliquot, all organisms were counted in a Bogorov chamber with a Leica stereomicroscope (MZ12), and specified to the lowest possible taxonomic level. Abundant taxa (>50 individuals per aliquot) were only counted from

these subsamples, while less abundant taxa were counted from entire net samples. Carbon biomass for copepods (*Calanus finmarchicus* and *Temora* sp.; separated into copepodites and adults, respectively) and hydrozoans (*Aglaantha* sp., *Clytia* sp., *Obelia* sp., and *Sarsia* sp.) was determined by manually picking specimen several times throughout the study. Sampled individuals were stored in tin cups, dried in an oven (60°C for at least 24h), and stored in a desiccator until measurement with an elemental analyzer (Euro EA-CN; Hekatech).

## 2.4 | Carbon export

Sediment traps mounted to the bottom of the mesocosms (i.e., covering the entire diameter of each mesocosm) ensured that the entire sinking fraction of particulate organic matter within the water column of the mesocosms was collected. Sinking particulate organic matter was sampled from the sediment traps (at 21 m depth) every second day and processed, following the procedures described in Boxhammer et al. (2016). Briefly, accumulated material was pumped through a silicon tube to the surface by applying a gentle vacuum (~300 mbar) with a manual pump. The particle suspension was collected in 5 L glass bottles and stored cool until subsequent processing in the land-based laboratories. The bulk samples were concentrated by centrifugation, frozen at -30°C, and freeze dried for 72 h before grinding them into a fine, homogenous powder. Small amounts of this processed material (1–2 mg) were then used for measuring particulate organic carbon (POC) content of the samples with an elemental analyzer (Euro EA-CN; Hekatech). Inorganic carbon content was removed with hydrochloric acid before analysis, to ensure that only organic carbon (biomass) was measured.

## 2.5 | Additional water column parameters

Water samples were collected every second day with 5 L water samplers (IWS, HYDRO-BIOS, Kiel) that permit depth-integrated sampling from the water column inside the mesocosms. Subsamples for chlorophyll *a* (chl *a*) were collected onto glass fiber filters (GF/F Whatman, pore size: 0.7 µm) and analyzed by reverse-phase high-performance liquid chromatography (HPLC) on a Thermo Scientific HPLC Ultimate 3000. Additionally, phytoplankton community composition was analyzed by flow cytometry (Accuri C6; BD Biosciences) from 650 µL subsamples. Individual populations were distinguished based on forward light scatter (FSC), chlorophyll *a* red fluorescence (FL3), and phycoerythrin orange fluorescence (FL2). Conversion of cell counts to carbon concentrations was done for each population by converting FSC to cell size (equivalent spherical diameter; ESD) following Taucher et al. (2017):

$$\text{ESD} = 0.0064 \times \text{FSC}^{0.5262}$$

Average ESD for the different groups were 2.0 µm (Pico), 8.2 µm (Nano), and 26.5 µm (Micro). ESD was then converted to spherical volume (*V*), which was used to estimate carbon using the formulation of Menden-Deuer and Lessard (2000):

$$C = 0.216 \times V^{0.939}$$

Subsamples for microzooplankton analyses via light microscopy were taken from the IWS every fourth day, filled into brown glass bottles (100 mL), and fixed with acidic Lugol's iodine (to a final concentration of ~1%) (Williams et al., 2016). Organisms in the size range of 20–200 µm were counted with the Utermöhl method (Utermöhl, 1958) and identified to genus level. Carbon content was estimated using geometric conversion to biovolume according to Hillebrand et al. (1999) and subsequent conversion using factors by Menden-Deuer and Lessard (2000) for dinoflagellates and Putt and Stoecker (1989) for ciliates. For more details, see Dörner et al. (2020).

Dissolved inorganic carbon (DIC) and total alkalinity (TA) samples were gently filtered directly after sampling (0.2 µm pore size) using a peristaltic pump, and stored at room temperature until measurement on the same day. DIC concentrations were determined based on infrared absorption using a LI-COR LI-7000 on an AIRICA system (MARIANDA, Kiel). TA was analyzed by potentiometric titration using a Metrohm 862 Compact Titrator and a 907 Titrando unit following the open-cell method described in Dickson et al. (2003). Partial pressure of aqueous CO<sub>2</sub> (*p*CO<sub>2</sub>) was then calculated with the Seacarb-R package (Gattuso et al., 2021) with the recommended default settings for carbonate dissociation constants (*K*<sub>1</sub> and *K*<sub>2</sub>) of Lueker et al. (2000).

## 2.6 | Carbon flux calculations for *O. dioica*

For the estimation of carbon fluxes mediated by grazing, as well as production of fecal pellets and houses by *O. dioica*, we applied two different approaches in order to account for possible variability between these methods.

In the first approach, we used the equations from the dynamic individual-based model of Lombard, Renaud, et al. (2009), in which rates of grazing, and production of houses and fecal pellets were computed with an allometric approach (i.e., as a function of body mass), also taking into account food concentration and temperature. These equations were applied to our data time series for food concentration, *O. dioica* abundances, average trunk length (which was converted to body mass using the equations in Lombard, Renaud, et al., 2009), and in situ temperature, using the parameter values given in Lombard, Renaud, et al. (2009). Following this model approach, house and fecal pellet production are primarily controlled by food intake (i.e., filtration rate), which is then divided into different compartments (houses, fecal pellets, respiration, as well as body structural biomass, gonads, and detritus stuck in the house), with the allocation among them being controlled by ingestion and assimilation efficiencies (which are, in turn, a function of food concentration).

In the second approach, we used constant values for grazing, production rates of houses and fecal pellets and their respective carbon content based on a literature synthesis (see Table 1 for values and references). The rate estimates were then applied to *O. dioica* abundances and body size or weight for the respective CO<sub>2</sub> treatment and day. For the literature review, we considered rates measured at comparable food concentrations (~80–130 µg C L<sup>-1</sup>), food regimes (i.e., prey

**TABLE 1** Compilation of rates and carbon conversions from literature.

<b>Grazing</b>		
Filtration rate [ $\mu\text{gC ind}^{-1} \text{ day}^{-1}$ ]	2.5–5.0	Acuña and Kiefer (2000)
Filtration rate [ $\mu\text{gC ind}^{-1} \text{ day}^{-1}$ ]	2.5–3.0	Troedsson et al. (2007)
C-specific filtration rate [ $\mu\text{gC} \mu\text{gC}^{-1} \text{ day}^{-1}$ ]	1.0–3.0	King (1982)
C-specific filtration rate [ $\mu\text{gC} \mu\text{gC}^{-1} \text{ day}^{-1}$ ]	3.6	Tiselius et al. (2003)
Value used here	2.0	$[\mu\text{gC} \mu\text{gC}^{-1} \text{ day}^{-1}]$
For body mass of 1.2–1.9 $\mu\text{gC ind}^{-1}$ (as found during this study)	2.4–3.8	$[\mu\text{gC ind}^{-1} \text{ day}^{-1}]$
<b>House production and carbon content</b>		
House production [ $\text{ind}^{-1} \text{ day}^{-1}$ ]	7.0	Hansen et al. (1996)
House production [ $\text{ind}^{-1} \text{ day}^{-1}$ ]	3.0 <sup>a</sup>	Sato et al. (2001)
House production [ $\text{ind}^{-1} \text{ day}^{-1}$ ]	2.0–5.0	Tiselius et al. (2003)
Value used here	3.0	$[\text{houses ind}^{-1} \text{ day}^{-1}]$
Fresh house carbon content [ $\mu\text{gC house}^{-1}$ ]	0.5–0.8	Sato et al. (2001)
Fresh house carbon as a fraction of body weight [ $\mu\text{gC} \mu\text{gC}^{-1}$ ]	0.15	Sato et al. (2001)
Discarded house carbon content [ $\mu\text{gC house}^{-1}$ ]	2.0–3.0	Allredge (2005)
Discarded house carbon as a fraction of body weight [ $\mu\text{gC} \mu\text{gC}^{-1}$ ]	0.58	Sato et al. (2001)
Discarded house carbon as a fraction of body weight [ $\mu\text{gC} \mu\text{gC}^{-1}$ ]	0.27 <sup>b</sup>	Sato et al. (2003)
Value used here	0.27	$[\mu\text{gC} \mu\text{gC}^{-1}]$
For a body mass of 1.2–1.9 $\mu\text{gC ind}^{-1}$ (as found during this study)	0.3–0.5	$[\mu\text{gC house}^{-1}]$
<b>Fecal pellet production and carbon content</b>		
Fecal pellet production [ $\text{ind}^{-1} \text{ h}^{-1}$ ]	2.0–5.0	Tiselius et al. (2003)
Fecal pellet production [ $\text{ind}^{-1} \text{ h}^{-1}$ ]	1.0–4.0	Selander and Tiselius et al. (2003)
Value used here	2.0	$[\text{ind}^{-1} \text{ h}^{-1}]$
Fecal pellet carbon content [ $\mu\text{gC pellet}^{-1}$ ]	0.032	González et al. (1994)
Fecal pellet carbon content [ $\mu\text{gC pellet}^{-1}$ ]	0.025 <sup>c</sup>	Lombard, Sciandra, et al. (2009)
Value used here	0.025	$[\mu\text{gC pellet}^{-1}]$

Note: When multiple values were available from literature, we estimated a mean value on the conservative end.

<sup>a</sup>Using the equation from Sato et al. (2001) for house renewal rate (HR) as a function of temperature ( $T$ ):  $\text{HR} = 0.0369 \times T - 0.210$ .

<sup>b</sup>Average value of four different *Oikopleura* species examined in Sato et al. (2003).

<sup>c</sup>Using equation (14) from Lombard, Renaud, et al. (2009) for fecal pellet carbon content (FPC) as a function of body weight (BW) and food concentration (F):  $\text{FPC} = 0.0651 \times \text{BW} \times \frac{F}{203 + F}$ .

size range of pico- and nanoplankton), and temperature (9–10°C) to those in our experiment. Since most rate measurements were conducted under idealized laboratory conditions, we chose numbers at the lower end for quantification of in situ rates in a natural plankton community for our carbon flux calculations. Rates of grazing, production of houses, and fecal pellets are highly dependent on body size and/or weight (Lombard, Renaud, et al., 2009; Sato et al., 2001). Thus, when such numbers were reported, we used them to calculate size- or mass-specific rates using our data on *O. dioica* body size distribution (measured every 4 days in each mesocosm) and corresponding carbon conversion based on Lombard, Renaud, et al. (2009). Thereby, the variability in body size of *O. dioica* during our study is taken into account

for carbon flux estimates. Fecal pellet production has been shown to also depend on food concentration (Selander & Tiselius, 2003), whereas house production is mostly controlled by appendicularian body weight and temperature, and largely independent of food concentrations (Fenaux, 1985; Sato et al., 2001). Note that some literature estimates for carbon content of houses refer to freshly produced appendicularian houses. However, under field conditions, discarded houses also contain egested fecal pellets and trapped particles (from previous filtration by the organism), as well as additional particles that are captured during sinking due to the stickiness of the mucous material (Allredge, 2005; Lombard, Sciandra, et al., 2009). Consequently, the carbon content of houses that were discarded some time ago can



reach up to two- to fivefold higher values than that of new houses (Sato et al., 2008). However, since we did not measure the carbon content of individual sinking houses in our study, we used an average of literature values. In contrast to the first, model-based approach, the rate estimates from this approach did not allocate a certain carbon budget into different pools, but yielded an independent estimate for each rate (grazing, house, and fecal pellet production).

Both approaches yielded very similar results, suggesting that the carbon flux estimates presented here are robust. Accordingly, values are given as the average of both approaches including the standard deviation. Based on these calculations, daily POC export by *O. dioica* reached up to almost twofold their population biomass. The contribution of discarded houses versus fecal pellets was on average 60% versus 40%.

### 3 | RESULTS AND DISCUSSION

#### 3.1 | Bloom dynamics of phytoplankton and *O. dioica*

The experiment started in the late phase of a diatom bloom, which soon declined and the produced biomass sank into the sediment traps. The fading diatom bloom coincided with a shift in the phytoplankton size structure. Microphytoplankton (mostly diatoms  $>20\mu\text{m}$ ) vanished while pico- ( $0.2\text{--}2\mu\text{m}$ ) and nanoplankton ( $2\text{--}20\mu\text{m}$ ) increased in biomass (Figure 1a). This shift from large diatoms to smaller phytoplankton (under both, ambient and high  $\text{CO}_2$  conditions) early in the experiment provided ideal boundary conditions for the subsequent growth of *O. dioica* populations (Figures 1c and 2b). The prey size spectrum of *O. dioica* is much broader than that found in most other planktivorous organisms (particularly in the micron- to sub-micron range; Dadon-Pilosof et al., 2023), with the optimum being in the range of 0.4%–2% of their own size (Flood, 1978; Lombard et al., 2011). For *O. dioica* in the size range observed in our study (Figure 2c), this corresponds to  $\sim 1\text{--}15\mu\text{m}$ , that is, most of the size range occupied by pico- and nanophytoplankton, both of which increased in biomass in the first 2 weeks of the experiment (Figure 3b,c).

The appendicularian *O. dioica* developed a distinct bloom, particularly under high  $\text{CO}_2$  conditions: The peak biomass of *O. dioica* was approximately twice as high in the high  $\text{CO}_2$  mesocosms ( $2.5$  vs.  $1.3\mu\text{gCL}^{-1}$ ) and occurred earlier (days 13–17) than under ambient conditions (day 21), thereby reflecting the treatment patterns observed in phytoplankton biomass that likely resulted from *O. dioica* grazing (less phytoplankton under high  $\text{CO}_2$ ) (Figure 1b,c). Coinciding with the *O. dioica* bloom, a major pulse of carbon export occurred under high  $\text{CO}_2$  conditions (days 17–19), reaching daily fluxes of up to  $10\mu\text{gCL}^{-1}$  (Figure 1d).

#### 3.2 | Competitive advantage of *O. dioica* under high $\text{CO}_2$

The marked amplification of the *O. dioica* bloom under high  $\text{CO}_2$  conditions raises the question for the underlying mechanism.

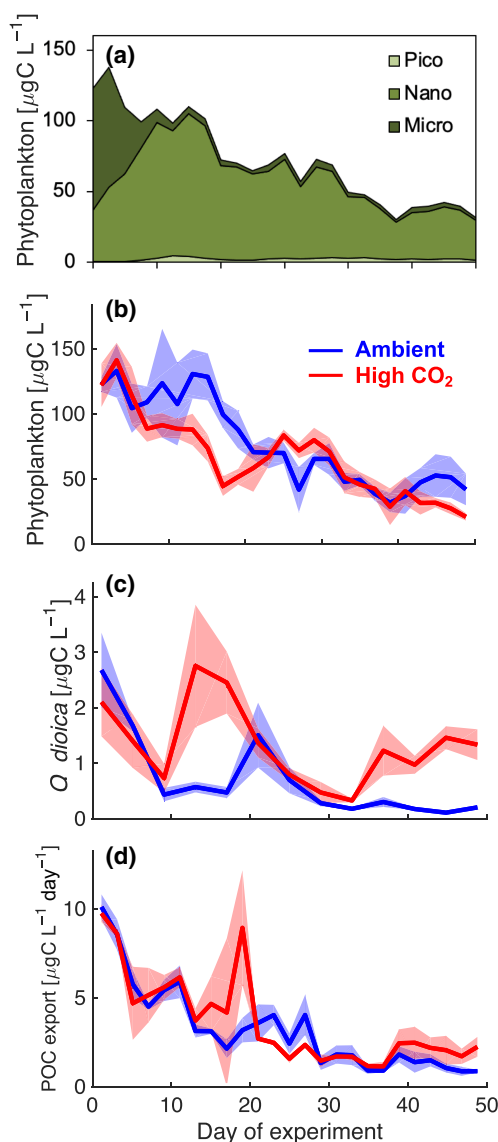


**FIGURE 1** (a) Biomass of phytoplankton (based on flow cytometry) in different size classes over the course of the study (average of all mesocosms). (b) Time series of biomass of phytoplankton and (c) *Oikopleura dioica*, as well as (d) particulate organic carbon (POC) export collected by sediment traps under the different  $\text{CO}_2$  conditions. Shown in (b–d) are average values of ambient (blue) and high  $\text{CO}_2$  (red) mesocosms, with shaded areas denoting standard deviations.

Based on the few existing  $\text{CO}_2$  perturbation studies on entire plankton communities, the common notion is that zooplankton responses to OA are primarily driven by  $\text{CO}_2$  effects on primary producers, which may then in turn indirectly affect heterotrophic organisms and food web structure (Riebesell et al., 2018; Sswat et al., 2018). In this study, we found strong evidence for a direct positive effect of elevated  $\text{CO}_2$  on *O. dioica*: The fecundity of *O. dioica* was significantly elevated under lower pH, with females producing  $278 (\pm 107)$  eggs under ambient and  $334 (\pm 14)$  eggs in the OA treatment, corresponding to a 20% increase of fecundity under high  $\text{CO}_2$  (Figure 2a). This finding is consistent with earlier

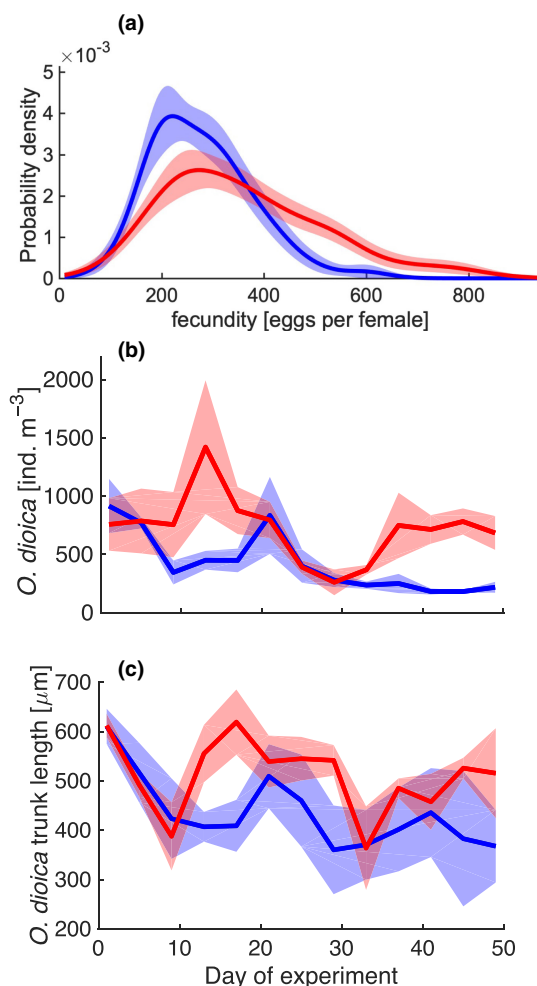


**FIGURE 2** Ecological performance of *Oikopleura dioica*: (a) fecundity of *O. dioica* females during the major bloom period until day 21, shown as probability density distributions with shaded areas denoting confidence intervals derived from bootstrapping. Abundance (b) and trunk length (c) of *O. dioica* during the mesocosm experiment, with shaded areas denoting standard deviations. Shown are ambient (blue) and high CO<sub>2</sub> (red) conditions.

physiological laboratory experiments with the same species, which found that enhanced digestion and assimilation efficiency at lower pH enhance fecundity of *O. dioica* (Bouquet et al., 2018). Moreover, low pH conditions not only increased average fecundity but also led to a shift in the frequency distribution of fecundity, with a much higher occurrence of females with very high egg production (>500 eggs per female) (Figure 2a).

The observed proliferation of *O. dioica* under high CO<sub>2</sub> conditions showed that these physiological responses translate into an increase in the competitive ability of *O. dioica* in their natural environment, accelerating reproduction and population growth of this species in pelagic plankton communities. Considering a generation time of *O. dioica* of about 10–12 days for in situ temperatures of 9–10°C (Bouquet, 2017; Lombard, Sciandra, et al., 2009), the observed boost in fecundity and reproduction can explain much of the bloom amplification under high CO<sub>2</sub> (faster development and

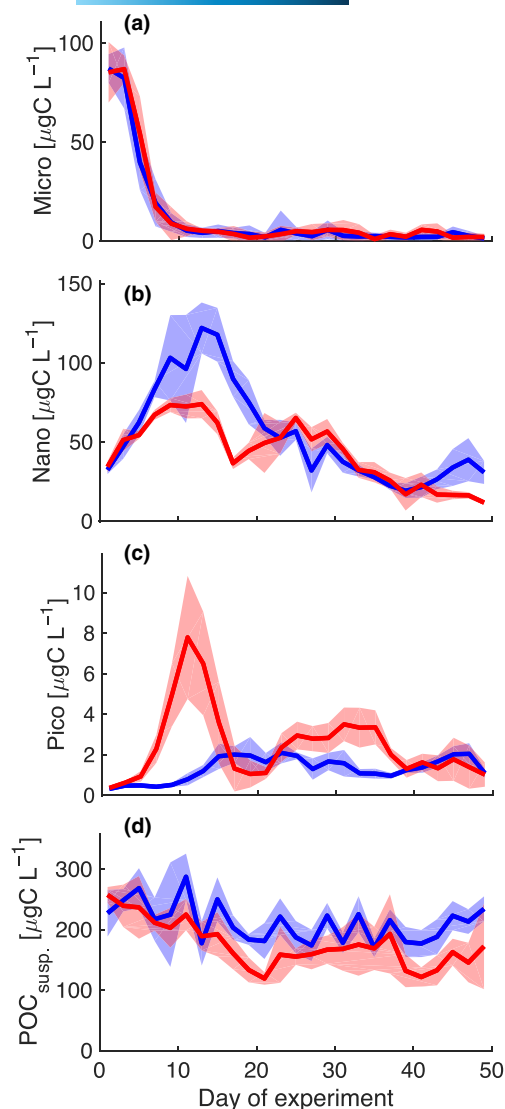


**FIGURE 3** Biomass of micro- (a), nano- (b), and picophytoplankton (c) and suspended particulate organic carbon (POC) in the water column (d). Shown are average values of ambient (blue) and high CO<sub>2</sub> (red) mesocosms, with shaded areas denoting standard deviations.

higher peak population size; Figure 2b). These findings are further corroborated by the larger body size of *O. dioica* individuals in the high CO<sub>2</sub> treatment, which likely also resulted from the beneficial physiological effects of lower pH on digestion and assimilation efficiency (Bouquet, 2017; Bouquet et al., 2018) (Figure 2c).

It should be noted that CO<sub>2</sub> conditions in our experiment were exceptionally high, representing future extreme events (Burger et al., 2020) and longer term acidification (Meinshausen et al., 2011), and thus not being representative of large-scale OA as projected for the 21st century. However, as earlier experimental work with *O. dioica* has shown that physiological effects of CO<sub>2</sub> on fecundity scale in a linear way (Bouquet et al., 2018), the general trend of our results should also hold true under more moderate levels of OA (with a proportionally reduced effect size).

### 3.3 | CO<sub>2</sub> responses of *O. dioica* and phytoplankton: Bottom-up versus top-down effects

The enhanced *O. dioica* biomass and associated changes in grazing were also reflected at the level of primary producers. Observed differences in *O. dioica* bloom patterns among ambient (later and lower peak) and high CO<sub>2</sub> conditions (earlier and higher peak) (Figure 2b) match remarkably well with the differences in total phytoplankton biomass (earlier and stronger decline under high CO<sub>2</sub>, Figure 1b,c) as well as suspended POC (Figure 3d).

Both pico- and nanoplankton both lie in the prey size range of *O. dioica* (Dadon-Pilosof et al., 2023; Lombard et al., 2011). Thus, either bottom-up or top-down pathways are conceivable for explaining the observed CO<sub>2</sub> effects on phytoplankton: On the one hand, physiological responses of pico- and nanoeukaryotes could have driven their increase/decrease under high CO<sub>2</sub>, thereby affecting *O. dioica* (and its treatment response) in a bottom-up manner. On the other hand, the treatment differences in *O. dioica* population dynamics (due to direct pH effects on physiology and fecundity) could have altered grazing pressure on pico- and nanophytoplankton, thereby shaping their observed CO<sub>2</sub> effects. Although it is difficult to disentangle these mechanisms with the available data (time series of standing stocks), a detailed analysis of temporal dynamics and treatment responses strongly supports the argument for a direct CO<sub>2</sub> effect on *O. dioica* and its top-down control.

The temporal patterns of picophytoplankton match with those of *O. dioica* (e.g., decline in picophytoplankton during *O. dioica* bloom under high CO<sub>2</sub>). However, as the biomass of picophytoplankton was relatively low (ambient: max. 2 µgC L<sup>-1</sup>, high CO<sub>2</sub>: max. 7 µgC L<sup>-1</sup>), it is insufficient to meet the estimated grazing demand of *O. dioica* (ambient: 17 µgC L<sup>-1</sup>, high CO<sub>2</sub>: 31 µgC L<sup>-1</sup>; see Figure 4). In contrast, the biomass of nanophytoplankton was more than an order of magnitude higher than that of picophytoplankton, thus likely constituting the major diet of *O. dioica*. Moreover, the temporal patterns of CO<sub>2</sub> effects on nanophytoplankton match strikingly well with those of *O. dioica* (see Figures 1c and 3b). In particular, lower nanophytoplankton during the *O. dioica* bloom under high CO<sub>2</sub> likely reflected enhanced top-down control of *O. dioica*, that is, a large portion of primary production was directly channeled into *O. dioica* grazing, thus preventing the buildup of biomass and a visible emergence of a nanophytoplankton bloom (i.e., the peak was “cut off”). Altogether, this suggests that the observed CO<sub>2</sub> effects on primary producers are the consequence of a direct positive effect of high CO<sub>2</sub> conditions on *O. dioica* and associated changes in top-down control.

### 3.4 | The role of *O. dioica* in carbon export and its response to high CO<sub>2</sub>

The important role of *O. dioica* in the food web was also reflected in carbon fluxes through the ecosystem. We observed a remarkable similarity of the temporal patterns and CO<sub>2</sub> effects between

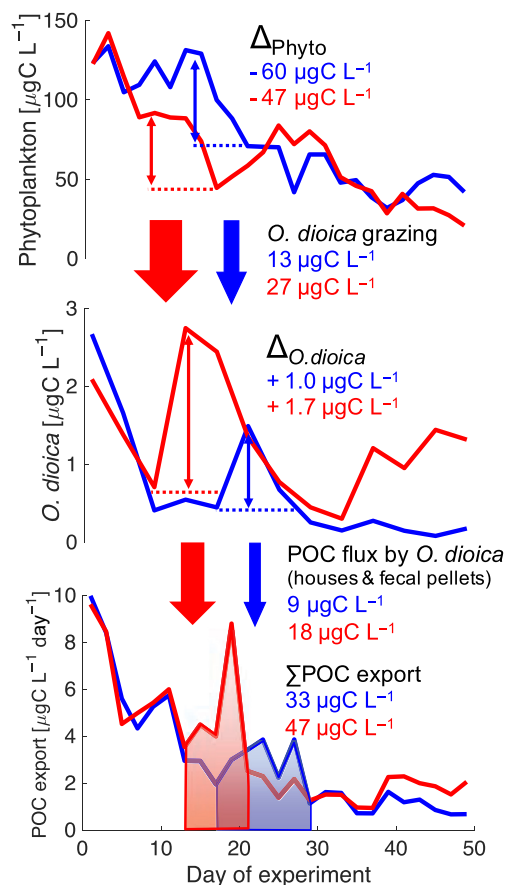


**FIGURE 4** Conceptual diagram illustrating the role of *Oikopleura dioica* for phytoplankton grazing and carbon export in the ambient (blue) and high (red) CO<sub>2</sub> mesocosms. Consumption of phytoplankton was computed for the respective bloom periods of *O. dioica* under ambient (17–25) and high CO<sub>2</sub> conditions (9–17), denoted by horizontal dashed lines and vertical arrows, and compared to the observed decrease in phytoplankton biomass during the same periods ( $\Delta_{\text{Phyto}}$ ). Similarly, vertical particulate organic carbon (POC) fluxes by *O. dioica* (from discarded houses and fecal pellets) were computed for the bloom period ( $\Delta_{\text{O. dioica}}$  denoting the peak build-up of biomass) and compared with observed POC export pulses that we attributed to the *O. dioica* bloom ( $\Sigma\text{POC export}$  for the days 17–27 and 13–21 under ambient and high CO<sub>2</sub> conditions, respectively).

*O. dioica* and export of POC from the water column, indicating that this species constituted a dominant driver of vertical carbon flux in our study (see Figures 1c,d and 3d). The major pulse of POC export in the high CO<sub>2</sub> mesocosms occurred on days 17–19, that is, directly after the bloom peak of *O. dioica*, reaching up to threefold higher daily fluxes than in the ambient mesocosms (Figure 1d). This suggests that the proliferation of *O. dioica* under high CO<sub>2</sub> (earlier and stronger bloom) enhanced the conversion of suspended POC (e.g., phytoplankton) into sinking particles, that is, fecal pellets and discarded feeding houses. A similar, but less pronounced pattern was also visible in the ambient treatment, where an intermittent period of elevated POC fluxes (days 19–27) coincided with a delayed and less pronounced *O. dioica* bloom (peak on day 21).



The in situ mesocosm approach allowed us to track the entire temporal development of an *O. dioica* bloom and POC export in a closed system, comprising a water column of ~20m depth. To quantitatively assess to what extent *O. dioica* was the main driver of observed patterns in phytoplankton biomass and carbon export, we conceived a simple model scheme of carbon fluxes mediated by *O. dioica*. Therefore, we used the temporal development of abundances and body size of *O. dioica* individuals to assess grazing rates on phytoplankton and production of sinking mucous houses and fecal pellets.

The derived flux estimates underline the key role of *O. dioica* in the food web and in driving carbon export, and particularly how these properties were enhanced under high CO<sub>2</sub> conditions (Figure 4): Estimated consumption of phytoplankton biomass via *O. dioica* grazing was  $12.6 \pm 0.1 \mu\text{gCL}^{-1}$  and  $26.6 \pm 2.0 \mu\text{gCL}^{-1}$  during the respective blooms under ambient and high CO<sub>2</sub> conditions, explaining ~20% and 60% of the simultaneous decrease in phytoplankton biomass ( $-60 \mu\text{gCL}^{-1}$  and  $-47 \mu\text{gCL}^{-1}$ , respectively). The remaining decrease of phytoplankton may be explained by microzooplankton, which displayed treatment responses matching predator-prey dynamics (i.e., elevated biomass under ambient conditions; Figure 6). The more prominent role of *O. dioica* in the food web under high CO<sub>2</sub> is also mirrored in its contribution to carbon export: Our estimated flux of POC export driven by *O. dioica* (discarded houses and fecal pellets) was notably enhanced in the high CO<sub>2</sub> mesocosms, reaching  $18.1 \pm 2.5 \mu\text{gCL}^{-1}$  compared to  $8.6 \pm 0.4 \mu\text{gCL}^{-1}$  ( $39 \pm 5\%$  and  $26 \pm 2\%$  of the observed total POC export, respectively). These results are in line with earlier studies on *O. dioica*, which found that the flux of discarded houses (mucous structure + contained non-ingested particles) and fecal pellets can reach several times the population biomass (Lombard, Sciandra, et al., 2009; Sato et al., 2001). Altogether, our flux estimates suggest that *O. dioica* substantially contributed to the observed enhancement of POC export under higher CO<sub>2</sub> conditions, which was elevated by 42%–64% compared to ambient conditions during the reference period (Figure 4). These calculations illustrate the outsized role of *O. dioica* in carbon export, particularly under high CO<sub>2</sub>.

Another treatment effect emerged starting around day 35, with once again elevated biomass of *O. dioica* and POC fluxes under high CO<sub>2</sub> conditions until the end of the study. However, the bloom was still developing at the end of the experiment, and the associated POC export pulse into the sediment traps remained incomplete, such that it was not possible to calculate the contribution of *O. dioica* in a similar manner to the major bloom and POC export event. Nevertheless, the imprint of *O. dioica* was still clearly detectable after several weeks: Cumulative carbon flux over the entire study period of 50 days was 14% higher under high CO<sub>2</sub> compared to ambient conditions (Figure 5a). Moreover, consistent with our estimates for the contribution of *O. dioica* to vertical POC fluxes, linear regression analysis indicated a significant ( $p = .011$ ) increase of POC export with *O. dioica* biomass (Figure 5b), underpinning the critical role of *O. dioica* as key driver

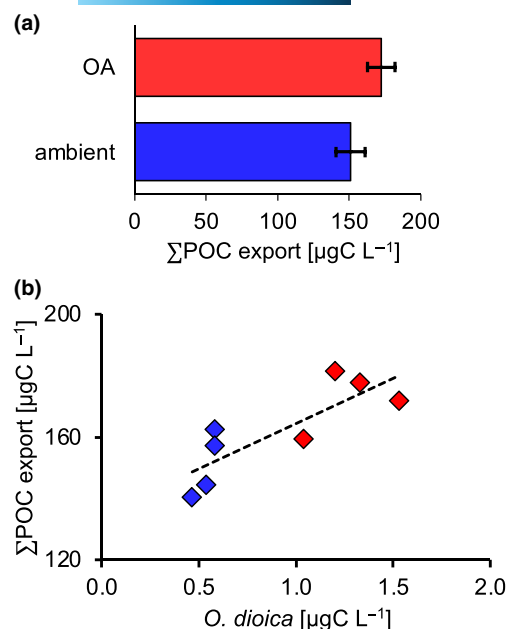


**FIGURE 5** (a) Cumulative particulate organic carbon (POC) export in the ambient (blue) and high CO<sub>2</sub> (red) treatment (error bars denote standard deviation). (b) Relationship between *Oikopleura dioica* and POC export as analyzed by linear regression ( $y = 0.0696x + 122.11$ ;  $p = .011$ ,  $R^2 = .69$ ), using *O. dioica* biomass (averaged over the study period for each mesocosm) and cumulative POC export (sum of POC collected by the sediment traps over the study period).

of POC export, and how this property was further enhanced by increasing CO<sub>2</sub>.

### 3.5 | The role of *O. dioica* compared to other zooplankton

The pronounced influence of *O. dioica* on phytoplankton dynamics and carbon fluxes may appear surprising, considering that the contribution of this species to total zooplankton biomass was rather small during our study (<5%, Figure 6).

A key factor for the outsized role of *O. dioica* in top-down control and carbon export probably lies in the particular ecological characteristics of appendicularians: These organisms are known for their extraordinarily high grazing rates, short generation times and particularly the continuous production and discarding of carbon-rich mucous houses, which can reach more than five times of an individual's body carbon per day (Hopcroft & Roff, 1995; Lombard, Sciandra, et al., 2009; Sato et al., 2008) (Table 1). These traits can explain the major findings of our study, particularly the bloom under high CO<sub>2</sub> conditions: *O. dioica* biomass increased more than threefold within 4 days, resulting in this species acting as the dominant vector for transferring primary production to carbon export during its short but intense bloom.

Further reasons for the disproportionately strong impact of *O. dioica* on carbon fluxes may lie in zooplankton community composition

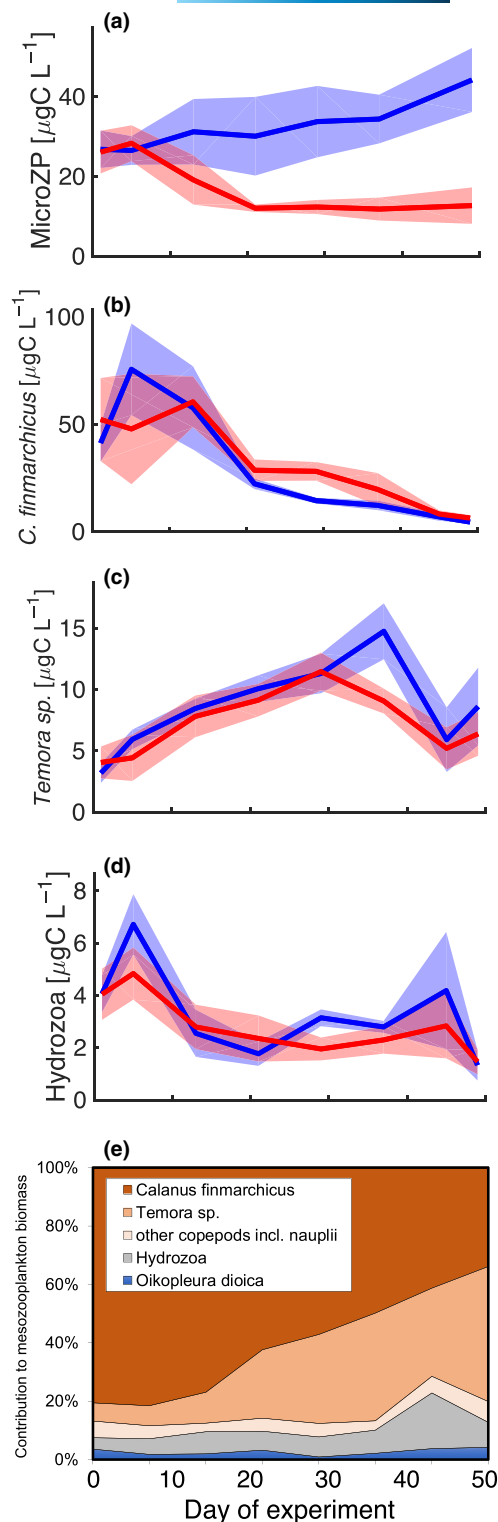


**FIGURE 6** Biomass of microzooplankton (a), the two dominant copepod species, *Calanus finmarchicus* (b) and *Temora* sp. (c), as well as hydrozoans (d). Shown are average values of ambient (blue) and high CO<sub>2</sub> (red) mesocosms, with shaded areas denoting standard deviations. Relative composition of mesozooplankton biomass by different species over the course of the experiment (average of all mesocosms) (e).

and food web structure. Indeed, none of the other zooplankton taxa (with a larger biomass) displayed treatment responses and/or temporal dynamics that could explain the observed patterns in

phytoplankton and carbon export (Figure 6), thus strengthening the argument for the key role of *O. dioica* in our experiment.

Mesozooplankton was dominated by the copepod species *C. finmarchicus* and *Temora* sp., as well as hydrozoans (Figure 6e). The dominant species *C. finmarchicus* declined after day 13 until the end of the study. This indicates that, after capitalizing from the diatom bloom, this species could not access the predominant prey size class (pico- and nanoplankton), or at least not as efficiently as *O. dioica*. Accordingly, the nutrition of *C. finmarchicus* likely had to occur via the microzooplankton link, which substantially reduced trophic transfer efficiency due to an additional trophic step (assuming ~10% transfer efficiency per trophic level) (Landry & Calbet, 2004). In contrast, *O. dioica* had the advantage of feeding directly on predominantly small primary producers (particularly nanophytoplankton), which are in its optimum prey size range (Flood, 1978; Lombard et al., 2011). The second-most important copepod species, *Temora* sp. increased in abundance for 4–5 weeks (Figure 6), indicating that *Temora* sp. could graze more efficiently in the size range of the pico- and nanoplankton during their blooms in the first half of the experiment (compared to *C. finmarchicus*). Although a treatment effect was detected on day 37 (lower biomass under high CO<sub>2</sub>), this occurred much too late to have played a role in the treatment effects on phytoplankton dynamics and POC export that we attribute to *O. dioica* (between days 10 and 27). The third largest contributor to mesozooplankton biomass were hydrozoans, consisting mostly of *Aglantha* sp., *Clytia* sp., *Obelia* sp. and *Sarsia* sp. As carnivorous predators, they are not expected to directly transfer phytoplankton into export. Furthermore, their biomass declined throughout the first half of the experiment and displayed no response to high CO<sub>2</sub> during the *O. dioica* bloom period and related POC export events. Thus, it seems unlikely that hydrozoans contributed to the observed temporal and treatment patterns of carbon export.

Besides mesozooplankton, we observed a high biomass of microzooplankton (Figure 6a), which were potentially a direct competitor to *O. dioica* for pico- and nanoplankton prey. Microzooplankton was composed of mixotrophic dinoflagellates (mainly *Ceratium* spp.) and heterotrophic ciliates (mainly *Strombidium* spp.). A detailed description of the data can be found in Dörner et al. (2020). Microzooplankton displayed a distinct response to high CO<sub>2</sub>, with three- to fourfold lower microzooplankton biomass than under ambient conditions (Figure 6). In theory, this pattern could either be (i) a cause of elevated *O. dioica* abundances (negative CO<sub>2</sub> effect diminishes microzooplankton, thereby leaving more phytoplankton prey for *O. dioica*) or (ii) a result of elevated *O. dioica* abundances (enhanced phytoplankton grazing by *O. dioica* reduces available prey for microzooplankton). However, the first scenario seems unlikely, as previous studies have not found evidence for direct physiological effects on microzooplankton (Aberle et al., 2013; Horn et al., 2015, 2016). Furthermore, the treatment patterns observed in microzooplankton (lower under high CO<sub>2</sub>) do not indicate alleviation of top-down control on phytoplankton (also lower under high CO<sub>2</sub>). Accordingly, the much more likely explanation is that the proliferation of *O. dioica* under high CO<sub>2</sub> triggered a trophic cascade, in which

enhanced grazing of *O. dioica* on pico- and nanoplankton reduced prey availability for microzooplankton and thus inhibited their population growth.

Altogether, none of the zooplankton taxa displayed temporal dynamics or treatment responses that could explain the observed CO<sub>2</sub> effects on phytoplankton and POC export (particularly the major flux event under high CO<sub>2</sub> between days 9 and 17). The favorable conditions of predator–prey coupling for *O. dioica* likely contributed to its decisive role of in driving carbon fluxes in our study.

## 4 | CONCLUSION

Our in situ mesocosm experiment allowed us to draw a detailed quantitative picture of carbon fluxes driven by *O. dioica*, revealing that this species can have disproportionately high contribution to carbon export even with a relatively low population biomass. Furthermore, our findings demonstrate that the importance of *O. dioica* as a driver of carbon export might further increase under OA. Low pH conditions as expected for future OA extreme events resulted in a distinct competitive advantage of *O. dioica* over other zooplankton: Beneficial effects of high CO<sub>2</sub> on the physiology (digestion, assimilation efficiency) and fecundity (egg production) of *O. dioica* enhanced its population growth and bloom development in a natural plankton community, thereby triggering trophic cascades, which opened a niche for *O. dioica* to play a key role in the trophic network. The resulting changes in phytoplankton population dynamics, food web structure and carbon export emphasize the high ecological and biogeochemical relevance of appendicularians.

## AUTHOR CONTRIBUTIONS

Jan Taucher was involved in conceptualization, investigation, methodology, formal analysis, data curation, visualization, writing—original draft. Anna Katharina Lechtenbörger was involved in investigation, formal analysis, data curation, writing—review and editing. Jean-Marie Bouquet was involved in methodology, data curation, writing—review and editing. Carsten Spisla was involved in investigation, formal analysis, writing—review and editing. Tim Boxhammer was involved in methodology, conceptualization, investigation. Fabrizio Minutolo was involved in investigation, formal analysis. Lennart Thomas Bach was involved in investigation, conceptualization, writing—review and editing. Kai T. Lohbeck investigation, formal analysis, writing—review and editing. Michael Sswat was involved in investigation, writing—review and editing. Isabel Dörner was involved in investigation. Stefanie M. H. Ismar-Rebitz was involved in investigation. Eric M. Thompson was involved in supervision, resources, funding acquisition. Ulf Riebesell was involved in conceptualization, investigation, supervision, resources, funding acquisition.

## ACKNOWLEDGMENTS

We thank all participants of the KOSMOS Norway 2015 experiment for maintenance and sampling of the mesocosm infrastructure. We

are grateful to the staff of the Marine Biological Station Espeland of the University of Bergen, in particular Tomas Sørli, for providing excellent infrastructure and daily support as well. We are grateful to the captains and crews of R/V Alkor (AL455), R/V Poseidon (POS486T), and R/V Håkon Mosby (2015627, 2015628) for the transportation and mooring of the mesocosm infrastructure. Funding for the study was provided through the German Research Foundation (DFG) Leibniz Award 2012 to U.R. and the DFG Excellence Cluster “The Future Ocean” and a grant from the Norwegian Research Council NFR-HK 204040 to E.M.T. Open Access funding enabled and organized by Projekt DEAL.

## CONFLICT OF INTEREST STATEMENT

The authors declare no competing interests.

## DATA AVAILABILITY STATEMENT

The data that support the findings of this study are openly available in the PANGAEA database: *O. dioica*, phytoplankton and POC export: <https://doi.org/10.1594/PANGAEA.962991> (Taucher et al., 2023). Other mesozooplankton: <https://doi.org/10.1594/PANGAEA.945306> (Spisla et al., 2022). Microzooplankton data: <https://doi.org/10.1594/PANGAEA.919632> (Haus et al., 2020).

## ORCID

Jan Taucher  <https://orcid.org/0000-0001-9944-0775>

Lennart Thomas Bach  <https://orcid.org/0000-0003-0202-3671>

Michael Sswat  <https://orcid.org/0000-0002-5957-4792>

## REFERENCES

- Aberle, N., Schulz, K. G., Stühr, A., Malzahn, A. M., Ludwig, A., & Riebesell, U. (2013). High tolerance of microzooplankton to ocean acidification in an Arctic coastal plankton community. *Biogeosciences*, 10(3), 1471–1481. <https://doi.org/10.5194/bg-10-1471-2013>
- Acuña, J. L., & Kiefer, M. (2000). Functional response of the appendicularian *Oikopleura dioica*. *Limnology and Oceanography*, 45(3), 608–618. <https://doi.org/10.4319/lo.2000.45.3.0608>
- Allredge, A. L. (2005). The contribution of discarded appendicularian houses to the flux of particulate organic carbon from oceanic surface waters. In G. Gorsky, M. J. Youngbluth, & D. Deibel (Eds.), *Response of marine ecosystems to global change: Ecological impact of appendicularians* (pp. 309–326). Contemporary Publishing International.
- Berline, L., Stemmann, L., Vichi, M., Lombard, F., & Gorsky, G. (2010). Impact of appendicularians on detritus and export fluxes: A model approach at DyFAMed site. *Journal of Plankton Research*, 33(6), 855–872. <https://doi.org/10.1093/plankt/fbq163>
- Bouquet, J.-M. (2017). *Response of the gelatinous zooplankton Oikopleura dioica to warmer, acidified seawater conditions* (Ph.D. thesis). University of Bergen.
- Bouquet, J.-M., Spriet, E., Troedsson, C., Otterå, H., Chourrout, D., & Thompson, E. M. (2009). Culture optimization for the emergent zooplanktonic model organism *Oikopleura dioica*. *Journal of Plankton Research*, 31(4), 359–370. <https://doi.org/10.1093/plankt/fbn132>
- Bouquet, J.-M., Troedsson, C., Novac, A., Reeve, M., Lechtenbörger, A. K., Massart, W., Massart, W., Skaar, K. S., Aasjord, A., Dupont, S., & Thompson, E. M. (2018). Increased fitness of a key appendicularian zooplankton species under warmer, acidified seawater conditions.

- PLoS One, 13(1), e0190625. <https://doi.org/10.1371/journal.pone.0190625>
- Boxhammer, T., Bach, L. T., Czerny, J., & Riebesell, U. (2016). Technical note: Sampling and processing of mesocosm sediment trap material for quantitative biogeochemical analysis. *Biogeosciences*, 13(9), 2849–2858. <https://doi.org/10.5194/bg-13-2849-2016>
- Boyd, P. W., Claustre, H., Levy, M., Siegel, D. A., & Weber, T. (2019). Multi-faceted particle pumps drive carbon sequestration in the ocean. *Nature*, 568(7752), 327–335. <https://doi.org/10.1038/s41586-019-1098-2>
- Burd, A. B., Buchan, A., Church, M., Landry, M. R., McDonnell, A. M. P., Passow, U., & Steinberg, D. K. (2016). *Towards a transformative understanding of the ocean's biological pump: Priorities for future research*. Report of the NSF biology of the biological pump workshop, February 19–20, 2016 (Hyatt Place New Orleans, New Orleans, LA). <https://doi.org/10.1575/1912/8263>
- Burger, F. A., John, J. G., & Frölicher, T. L. (2020). Increase in ocean acidity variability and extremes under increasing atmospheric CO<sub>2</sub>. *Biogeosciences*, 17(18), 4633–4662. <https://doi.org/10.5194/bg-17-4633-2020>
- Dadon-Pilosof, A., Conley, K., Lombard, F., Sutherland, K. R., Genin, A., Richter, M., Glöckner, F. O., & Yahel, G. (2023). Differential clearance rates of microbial phylotypes by four appendicularian species. *Marine Ecology Progress Series*, 706, 73–89.
- Desmet, F., Gruber, N., Köhn, E. E., Münnich, M., & Vogt, M. (2022). Tracking the space-time evolution of ocean acidification extremes in the California current system and Northeast Pacific. *Journal of Geophysical Research: Oceans*, 127(5), e2021JC018159. <https://doi.org/10.1029/2021JC018159>
- Dickson, A. G., Afghan, J. D., & Anderson, G. C. (2003). Reference materials for oceanic CO<sub>2</sub> analysis: A method for the certification of total alkalinity. *Marine Chemistry*, 80(2–3), 185–197. [https://doi.org/10.1016/s0304-4203\(02\)00133-0](https://doi.org/10.1016/s0304-4203(02)00133-0)
- Dörner, I., Hauss, H., Aberle, N., Lohbeck, K., Spisla, C., Riebesell, U., & Ismar-Rebittz, S. M. H. (2020). Ocean acidification impacts on biomass and fatty acid composition of a post-bloom marine plankton community. *Marine Ecology Progress Series*, 647, 49–64.
- Fenaux, R. (1985). Rhythm of secretion of oikopleurid's houses. *Bulletin of Marine Science*, 37(2), 498–503.
- Flood, P. R. (1978). Filter characteristics of appendicularian food catching nets. *Experientia*, 34(2), 173–175. <https://doi.org/10.1007/BF01944659>
- Gattuso, J.-P., Epitalon, J.-M., Lavigne, H., & Orr, J. (2021). *Seacarb: Seawater carbonate chemistry*. R package version 3.3.0. <http://CRAN.R-project.org/package=seacarb>
- Goldenberg, S. U., Nagelkerken, I., Marangon, E., Bonnet, A., Ferreira, C. M., & Connell, S. D. (2018). Ecological complexity buffers the impacts of future climate on marine consumers. *Nature Climate Change*, 8(3), 229–233. <https://doi.org/10.1038/s41558-018-0086-0>
- González, H. E., González, S. R., & Brummer, G.-J. A. (1994). Short-term sedimentation pattern of zooplankton, faeces and microplankton at a permanent station in the Bjørnafjorden (Norway) during April–May 1992. *Marine Ecology Progress Series*, 105(1/2), 31–45.
- Gorsky, G., & Fenaux, R. (1998). The role of appendicularia in marine food webs. In Q. Bone (Ed.), *The biology of pelagic Tunicates* (pp. 161–169). Oxford University Press.
- Gruber, N., Boyd, P. W., Frölicher, T. L., & Vogt, M. (2021). Biogeochemical extremes and compound events in the ocean. *Nature*, 600(7889), 395–407. <https://doi.org/10.1038/s41586-021-03981-7>
- Hansen, J. L. S., Kiorboe, T., & Alldredge, A. L. (1996). Marine snow derived from abandoned larvacean houses: Sinking rates, particle content and mechanisms of aggregate formation. *Marine Ecology Progress Series*, 141(1–3), 205–215. <https://doi.org/10.3354/meps141205>
- Hauri, C., Gruber, N., McDonnell, A. M. P., & Vogt, M. (2013). The intensity, duration, and severity of low aragonite saturation state events on the California continental shelf. *Geophysical Research Letters*, 40(13), 3424–3428. <https://doi.org/10.1002/grl.50618>
- Hauss, H., Ismar, S. M., Dörner, I., & Aberle, N. (2020). Phytoplankton and microzooplankton biomass in the KOSMOS Experiment Bergen 2015. PANGAEA.
- Hillebrand, H., Dürselen, C.-D., Kirschtel, D., Pollinger, U., & Zohary, T. (1999). Biovolume calculation for pelagic and benthic microalgae. *Journal of Phycology*, 35(2), 403–424. <https://doi.org/10.1046/j.1529-8817.1999.3520403.x>
- Hopcroft, R. R., & Roff, J. C. (1995). Zooplankton growth rates: Extraordinary production by the larvacean *Oikopleura dioica* in tropical waters. *Journal of Plankton Research*, 17(2), 205–220. <https://doi.org/10.1093/plankt/17.2.205>
- Hopcroft, R. R., & Roff, J. C. (1998). Production of tropical larvaceans in Kingston harbour, Jamaica: Are we ignoring an important secondary producer? *Journal of Plankton Research*, 20(3), 557–569. <https://doi.org/10.1093/plankt/20.3.557>
- Horn, H. G., Boersma, M., Garzke, J., Löder, M. G. J., Sommer, U., & Aberle, N. (2015). Effects of high CO<sub>2</sub> and warming on a Baltic Sea microzooplankton community. *ICES Journal of Marine Science*, 73(3), 772–782. <https://doi.org/10.1093/icesjms/fsv198>
- Horn, H. G., Sander, N., Stühr, A., Alguero-Muñiz, M., Bach, L. T., Löder, M. G. J., Boersma, M., Riebesell, U., & Aberle, N. (2016). Low CO<sub>2</sub> sensitivity of microzooplankton communities in the Gullmar Fjord, Skagerrak: Evidence from a long-term mesocosm study. *PLoS One*, 11(11), e0165800. <https://doi.org/10.1371/journal.pone.0165800>
- Jaspers, C., Hopcroft, R. R., Kjørboe, T., Lombard, F., López-Urrutia, Á., Everett, J. D., & Richardson, A. J. (2023). Gelatinous larvacean zooplankton can enhance trophic transfer and carbon sequestration. *Trends in Ecology & Evolution*, 38(10), 980–993. <https://doi.org/10.1016/j.tree.2023.05.005>
- King, K. R. (1982). The population biology of the larvacean *Oikopleura dioica* in enclosed water columns. In G. D. Grice & M. R. Reeve (Eds.), *Marine mesocosms: Biological and chemical research in experimental ecosystems* (pp. 341–351). Springer.
- Kwiatkowski, L., & Orr, J. C. (2018). Diverging seasonal extremes for ocean acidification during the twenty-first century. *Nature Climate Change*, 8(2), 141–145. <https://doi.org/10.1038/s41558-017-0054-0>
- Landry, M. R., & Calbet, A. (2004). Microzooplankton production in the oceans. *ICES Journal of Marine Science*, 61(4), 501–507. <https://doi.org/10.1016/j.icesjms.2004.03.011>
- Lombard, F., Guidi, L., & Kjørboe, T. (2013). Effect of type and concentration of ballasting particles on sinking rate of marine snow produced by the appendicularian *Oikopleura dioica*. *PLoS One*, 8(9), e75676. <https://doi.org/10.1371/journal.pone.0075676>
- Lombard, F., Renaud, F., Sainsbury, C., Sciadra, A., & Gorsky, G. (2009). Appendicularian ecophysiology I: Food concentration dependent clearance rate, assimilation efficiency, growth and reproduction of *Oikopleura dioica*. *Journal of Marine Systems*, 78(4), 606–616. <https://doi.org/10.1016/j.jmarsys.2009.01.004>
- Lombard, F., Sciadra, A., & Gorsky, G. (2009). Appendicularian ecophysiology. II. Modeling, nutrition, metabolism, growth and reproduction of the appendicularian *Oikopleura dioica*. *Journal of Marine Systems*, 78(4), 617–629. <https://doi.org/10.1016/j.jmarsys.2009.01.005>
- Lombard, F., Selander, E., & Kjørboe, T. (2011). Active prey rejection in the filter-feeding appendicularian *Oikopleura dioica*. *Limnology and Oceanography*, 56(4), 1504–1512. <https://doi.org/10.4319/lo.2011.56.4.1504>
- Lueker, T. J., Dickson, A. G., & Keeling, C. D. (2000). Ocean pCO<sub>2</sub> calculated from dissolved inorganic carbon, alkalinity, and equations for K<sub>1</sub> and K<sub>2</sub>: Validation based on laboratory measurements of CO<sub>2</sub> in gas and seawater at equilibrium. *Marine Chemistry*, 70(1–3), 105–119. [https://doi.org/10.1016/s0304-4203\(00\)00022-0](https://doi.org/10.1016/s0304-4203(00)00022-0)
- Luo, J. Y., Condon, R. H., Stock, C. A., Duarte, C. M., Lucas, C. H., Pitt, K. A., & Cowen, R. K. (2020). Gelatinous zooplankton-mediated



- carbon flows in the global oceans: A data-driven modeling study. *Global Biogeochemical Cycles*, 34(9), e2020GB006704. <https://doi.org/10.1029/2020GB006704>
- Luo, J. Y., Grassian, B., Tang, D., Irlsson, J.-O., Greer, A. T., Guigand, C. M., McClatchie, S., & Cowen, R. K. (2014). Environmental drivers of the fine-scale distribution of a gelatinous zooplankton community across a mesoscale front. *Marine Ecology Progress Series*, 510, 129–149. <https://doi.org/10.3354/meps10908>
- Luo, J. Y., Stock, C. A., Henschke, N., Dunne, J. P., & O'Brien, T. D. (2022). Global ecological and biogeochemical impacts of pelagic tunicates. *Progress in Oceanography*, 205, 102822. <https://doi.org/10.1016/j.pcean.2022.102822>
- Meinshausen, M., Smith, S. J., Calvin, K., Daniel, J. S., Kainuma, M. L. T., Lamarque, J. F., Matsumoto, K., Montzka, S., Raper, S., Riahi, K., Thomson, A., Velders, G., & van Vuuren, D. P. P. (2011). The RCP greenhouse gas concentrations and their extensions from 1765 to 2300. *Climatic Change*, 109(1), 213–241. <https://doi.org/10.1007/s10584-011-0156-z>
- Menden-Deuer, S., & Lessard, E. J. (2000). Carbon to volume relationships for dinoflagellates, diatoms, and other protist plankton. *Limnology and Oceanography*, 45(3), 569–579.
- Nakamura, Y., Suzuki, K., Suzuki, S.-Y., & Hiromi, J. (1997). Production of *Oikopleura dioica* (appendicularia) following a picoplankton 'bloom' in a eutrophic coastal area. *Journal of Plankton Research*, 19(1), 113–124. <https://doi.org/10.1093/plankt/19.1.113>
- Putt, M., & Stoecker, D. K. (1989). An experimentally determined carbon-volume ratio for marine "oligotrichous" ciliates from estuarine and coastal waters. *Limnology and Oceanography*, 34(6), 1097–1103.
- Questel, J. M., Clarke, C., & Hopcroft, R. R. (2013). Seasonal and inter-annual variation in the planktonic communities of the northeastern Chukchi Sea during the summer and early fall. *Continental Shelf Research*, 67, 23–41. <https://doi.org/10.1016/j.csr.2012.11.003>
- Remsen, A., Hopkins, T. L., & Samson, S. (2004). What you see is not what you catch: A comparison of concurrently collected net, optical plankton counter, and shadowed image particle profiling evaluation recorder data from the Northeast Gulf of Mexico. *Deep Sea Research Part I: Oceanographic Research Papers*, 51(1), 129–151. <https://doi.org/10.1016/j.dsr.2003.09.008>
- Riebesell, U., Aberle-Malzahn, N., Achterberg, E. P., Alguero-Muniz, M., Alvarez-Fernandez, S., Aristegui, J., Bach, L. T., Boersma, M., Boxhammer, T., Guan, W., Haunost, M., Horn, H. G., Löscher, C. R., Ludwig, A., Spisla, C., Sswat, M., Stange, P., & Taucher, J. (2018). Toxic algal bloom induced by ocean acidification disrupts the pelagic food web. *Nature Climate Change*, 8(12), 1082. <https://doi.org/10.1038/s41558-018-0344-1>
- Riebesell, U., Czerny, J., von Brockel, K., Boxhammer, T., Budenbender, J., Deckelnick, M., Fischer, M., Hoffmann, D., Krug, S. A., Lentz, U., & Schulz, K. G. (2013). Technical note: A mobile sea-going mesocosm system – new opportunities for ocean change research. *Biogeosciences*, 10(3), 1835–1847. <https://doi.org/10.5194/bg-10-1835-2013>
- Sato, R., Ishibashi, Y., Tanaka, Y., Ishimaru, T., & Dagg, M. J. (2008). Productivity and grazing impact of *Oikopleura dioica* (Tunicata, Appendicularia) in Tokyo Bay. *Journal of Plankton Research*, 30(3), 299–309. <https://doi.org/10.1093/plankt/fbn001>
- Sato, R., Tanaka, Y., & Ishimaru, T. (2001). House production by *Oikopleura dioica* (Tunicata, Appendicularia) under laboratory conditions. *Journal of Plankton Research*, 23(4), 415–423. <https://doi.org/10.1093/plankt/23.4.415>
- Sato, R., Tanaka, Y., & Ishimaru, T. (2003). Species-specific house productivity of appendicularians. *Marine Ecology Progress Series*, 259, 163–172.
- Schartau, M., Landry, M. R., & Armstrong, R. A. (2010). Density estimation of plankton size spectra: A reanalysis of IronEx II data. *Journal of Plankton Research*, 32(8), 1167–1184. <https://doi.org/10.1093/plankt/fbq072>
- Selander, E., & Tiselius, P. (2003). Effects of food concentration on the behaviour of *Oikopleura dioica*. *Marine Biology*, 142(2), 263–270.
- Spisla, C., Taucher, J., Bach, L. T., Haunost, M., Boxhammer, T., King, A. L., Jenkins, B. D., Wallace, J. R., Ludwig, A., Meyer, J., Stange, P., Minutolo, F., Lohbeck, K. T., Nauendorf, A., Kalter, V., Lischka, S., Sswat, M., Dörner, I., Ismar-Rebitz, S. M. H., ... Riebesell, U. (2021). Extreme levels of ocean acidification restructure the plankton community and biogeochemistry of a temperate coastal ecosystem: A mesocosm study. *Frontiers in Marine Science*, 7(1240), 11157. <https://doi.org/10.3389/fmars.2020.611157>
- Spisla, C., Taucher, J., Sswat, M., Clemmesen, C., & Riebesell, U. (2022). KOSMOS Bergen 2015 mesocosm study: *Hydrozoa*, *C. harengus*, and *Copepoda* abundances and biomasses. PANGAEA.
- Sswat, M., Stiasny, M. H., Taucher, J., Alguero-Muñoz, M., Bach, L. T., Jutfelt, F., Riebesell, U., & Clemmesen, C. (2018). Food web changes under ocean acidification promote herring larvae survival. *Nature Ecology & Evolution*, 2, 836–840. <https://doi.org/10.1038/s41558-018-0514-6>
- Steinberg, D. K., Stamieszkin, K., Maas, A. E., Durkin, C. A., Passow, U., Estapa, M. L., Omand, M. M., McDonnell, A. M. P., Karp-Boss, L., Galbraith, M., & Siegel, D. A. (2023). The outsized role of Salps in carbon export in the subarctic Northeast Pacific Ocean. *Global Biogeochemical Cycles*, 37(1), e2022GB007523. <https://doi.org/10.1029/2022GB007523>
- Stone, J. P., & Steinberg, D. K. (2016). Salp contributions to vertical carbon flux in the Sargasso Sea. *Deep Sea Research Part I: Oceanographic Research Papers*, 113, 90–100. <https://doi.org/10.1016/j.dsr.2016.04.007>
- Taucher, J., Bach, L. T., Boxhammer, T., Nauendorf, A., Consortium, T. G. C. K., Achterberg, E. P., Alguero-Muñoz, M., Aristegui, J., Czerny, J., Esposito, M., Guan, W., Haunost, M., Horn, H. G., Ludwig, A., Meyer, J., Spisla, C., Sswat, M., Stange, P., & Riebesell, U. (2017). Influence of ocean acidification and deep water upwelling on oligotrophic plankton communities in the subtropical North Atlantic: Insights from an in situ mesocosm study. *Frontiers in Marine Science*, 4, 85. <https://doi.org/10.3389/fmars.2017.00085>
- Taucher, J., Boxhammer, T., Bach, L. T., Paul, A. J., Schartau, M., Stange, P., & Riebesell, U. (2020). Changing carbon-to-nitrogen ratios of organic-matter export under ocean acidification. *Nature Climate Change*, 11, 52–57. <https://doi.org/10.1038/s41558-020-00915-5>
- Taucher, J., Lechtenböcker, A. K., Lohbeck, K. T., Spisla, C., Boxhammer, T., & Minutolo, F. (2023). *Oikopleura dioica*, phytoplankton, and carbon export during the KOSMOS Bergen mesocosm experiment on ocean acidification. (Raunefjord, Norway, 2015).
- Tiselius, P., Petersen, J., Nielsen, T., Maar, M., Møller, E., Satapoomin, S., Tönnesson, K., Zervoudaki, S., Christou, E., Giannakourou, A., Sell, A. F., & Vargas, C. (2003). Functional response of *Oikopleura dioica* to house clogging due to exposure to algae of different sizes. *Marine Biology*, 142(2), 253–261. <https://doi.org/10.1007/s00227-002-0961-z>
- Troedsson, C., Bouquet, J.-M., Lobon, C. M., Novac, A., Nejtgaard, J. C., Dupont, S., Bosak, S., Jakobsen, H., Romanova, N., Pankoke, L., & Thompson, E. M. (2013). Effects of ocean acidification, temperature and nutrient regimes on the appendicularian *Oikopleura dioica*: A mesocosm study. *Marine Biology*, 160(8), 2175–2187. <https://doi.org/10.1007/s00227-012-2137-9>
- Troedsson, C., Frischer, M. E., Nejtgaard, J. C., & Thompson, E. M. (2007). Molecular quantification of differential ingestion and particle trapping rates by the appendicularian *Oikopleura dioica* as a function of prey size and shape. *Limnology and Oceanography*, 52(1), 416–427. <https://doi.org/10.4319/lo.2007.52.1.0416>
- Utermöhl, H. (1958). *Zur Vervollkommenung der quantitativen Phytoplankton-Methodik*. Stuttgart.
- Vargas, C. A., Tönnesson, K., Sell, A., Maar, M., Møller, E. F., Zervoudaki, T., Giannakourou, A., Christou, E., Satapoomin, S., Petersen, J. K., Nielsen, T. G., & Petersen, J. K. (2002). Importance of copepods



- versus appendicularians in vertical carbon fluxes in a Swedish fjord. *Marine Ecology Progress Series*, 241, 125–138.
- Volk, T., & Hoffert, M. I. (1985). Ocean carbon pumps: Analysis of relative strengths and efficiencies in ocean-driven atmospheric CO<sub>2</sub> changes. In E. T. Sundquist & W. S. Broecker (Eds.), *The carbon cycle and atmospheric CO<sub>2</sub>: Natural variations Archean to present* (Vol. 32, pp. 99–110). American Geophysical Union. <https://doi.org/10.1029/GM032p0099>
- Williams, O. J., Beckett, R. E., & Maxwell, D. L. (2016). Marine phytoplankton preservation with Lugol's: A comparison of solutions. *Journal of Applied Phycology*, 28(3), 1705–1712. <https://doi.org/10.1007/s10811-015-0704-4>
- Wilson, S. E., Ruhl, H. A., & Smith, K. L. (2013). Zooplankton fecal pellet flux in the abyssal Northeast Pacific: A 15 year time-series study. *Limnology and Oceanography*, 58(3), 881–892. <https://doi.org/10.4319/lo.2013.58.3.0881>
- Winder, M., Bouquet, J.-M., Rafael Bermúdez, J., Berger, S. A., Hansen, T., Brandes, J., Sazhin, A. F., Nejtgaard, J. C., Båmstedt, U., Jakobsen, H. H., Dutz, J., Frischer, M. E., Troedsson, C., & Thompson, E. M. (2017). Increased appendicularian zooplankton alter carbon cycling under warmer more acidified ocean conditions. *Limnology and Oceanography*, 62(4), 1541–1551. <https://doi.org/10.1002/lno.10516>

**How to cite this article:** Taucher, J., Lechtenböcker, A. K., Bouquet, J.-M., Spisla, C., Boxhammer, T., Minutolo, F., Bach, L. T., Lohbeck, K. T., Sswat, M., Dörner, I., Ismar-Rebitz, S. M. H., Thompson, E. M., & Riebesell, U. (2024). The appendicularian *Oikopleura dioica* can enhance carbon export in a high CO<sub>2</sub> ocean. *Global Change Biology*, 30, e17020. <https://doi.org/10.1111/gcb.17020>